Spontaneous Formation of Core/Shell Bimetallic Nanoparticles: A Calorimetric Study

Naoki Toshima,*,† Masao Kanemaru,† Yukihide Shiraishi,† and Yoshikata Koga‡

Department of Materials Science and Environmental Engineering, Tokyo University of Science, Yamaguchi, Onoda-shi, Yamaguchi, 756-0884, Japan, and Department of Chemistry, The University of British Columbia, 2036 Main Mall, Vancouver, B.C., Canada V6T 1Z1

Received: March 17, 2005; In Final Form: July 7, 2005

We showed recently that low entropy core/shell structured nanoparticles form spontaneously from the physical mixture of a dispersion of Ag nanoparticles and that of another noble metal (Rh, Pd, or Pt) at room temperature. Here we use isothermal titration calorimetry (ITC) and show that the initial step of such a spontaneous process is strongly exothermic. When the alcohol dispersion of poly(*N*-vinyl-2-pyrrolidone) (PVP)-protected Rh nanoparticles (average diameter 2.3 nm) was titrated into the alcoholic dispersion of PVP-protected Ag nanoparticles, a strong exothermic enthalpy change, ΔH, was observed: $\Delta H = -908$ kJ/mol for Ag(S) nanoparticle (average diameter 10.8 nm) and -963 kJ/mol for Ag(L) nanoparticles (average diameter 22.5 nm). The strength of interaction increases in the order of Rh/Ag > Pd/Ag > Pt/Ag. This strong exothermic interaction is considered as a driving force to from low entropy bimetallic nanoparticles by simple mixing of two kinds of monometallic nanoparticles. We show also that exothermic interactions occur between a pair of noble metal nanoparticles themselves by using ITC.

Introduction

Nanoparticles of noble metal have attracted much attention of late due to their wide applicability in "nanotechnology" or "nanobiotechnology". They show some remarkable characteristics in optical, electrical, magnetic, physicochemical, and chemical properties and in some combinations of the above properties.[1−7] More recently, particular interests are focused in bimetallic nanoparticles, which exhibit unique characteristics that are not just the addition of the two properties of the constituent metals.[8−10] For example, Pd/Pt bimetallic nanoparticles have much higher catalytic activity than the mixture of the corresponding monometallic nanoparticles.[8,9,11,12] Bimetallic nanoparticles are known to take various kinds of structure: from a high entropy situation of a solid solution random alloy to such a low entropy product as a cluster-in-cluster, a layered compound, a heterobondphilic structure, and a core/shell structure.[9,10,13,14]

In 1991, we showed for the first time[15] that the Pt/Pd bimetallic nanoparticles prepared by reduction of a solution containing both metal ions with refluxing ethanol were in the form of core/shell structure. The key evidence for this structure was obtained by EXAFS.[15,16] Since then, a number of examples were reported that are of core/shell form: Au/Pd[17] and Au/Pt[18] by the same reduction method of refluxing ethanol, Au/Pd[19,20] by sonochemical reaction, Au/Pd and Au/Pt by reduction with phosphotungstic acid,[21] Au/Pt on TiO_2 by subsequent photodeposition,[22] and Pt/Au by photoreduction and subsequent γ-radiolytic decomposition.[23] We have also presented a novel method to control the core/shell structure[24] whereby metal hydride nanoparticles formed by H_2 adsorption were used to reduce other metal ions.

Recently, we surprisingly found[25] that bimetallic nanoparticles of core/shell structure formed spontaneously on physically mixing PVP-protected Ag nanoparticles with PVP-protected Rh nanoparticles in solution, although the resulting bimetallic nanoparticles do not show the core/shell structure as clearly as typical cases mentioned above. This was evident also by TEM observation,[25] and hence we call this case as having a pseudo-core/shell structure. It is indeed surprising that such a low-entropy, well-organized structure forms automatically just by physical mixing. The process is depicted in Figure 1. We call this an example of self-organization.[26]

Self-organization is generally realized when a system in question is far away from an equilibrium and there is necessarily a positive or negative feed-back loop in rate steps.[27]

Whether colloidal systems are in equilibrium states is a fundamental question and remains unanswered. However, if a system is isolated due to some kinetic barriers it could be regarded in an equilibrium locally.[28,29] Here we treat the present bimetallic core/shell nanoparticles as being in a stable equilibrium state. Thus, for this low-entropy situation to be realized, there must be a strong exothermic motivation.

In the present work, we make an attempt at determining enthalpy gain, if any, in mixing two sets of PVP-protected nanoparticles. Isothermal titration calorimetry (ITC) is a sensitive technique capable of measuring minute heats of interaction between two reacting species. It has been applied with great success for studies of interactions among biomolecules in dilute aqueous solutions.[30−34]

There are recent studies applying ITC for interactions between Au nanoparticles with biomolecules.[35,36] We apply here the ITC technique to study enthalpic interactions between nanoparticles. We believe this is the first attempt for determining colloidal reactions. We have submitted a brief communication[37] to the Proceedings to the 3rd International Symposium on the Frontiers of Calorimetry and Thermal Analysis covering a part of the study presented here.

* Address correspondence to this author. Phone: +81-836-88-4561. Fax: +81-836-88-4567. E-mail: toshima@ed.yama.tus.ac.jp.
† Tokyo University of Science, Yamaguchi.
‡ The University of British Columbia.

10.1021/jp051400h CCC: $30.25
Published on Web 08/10/2005

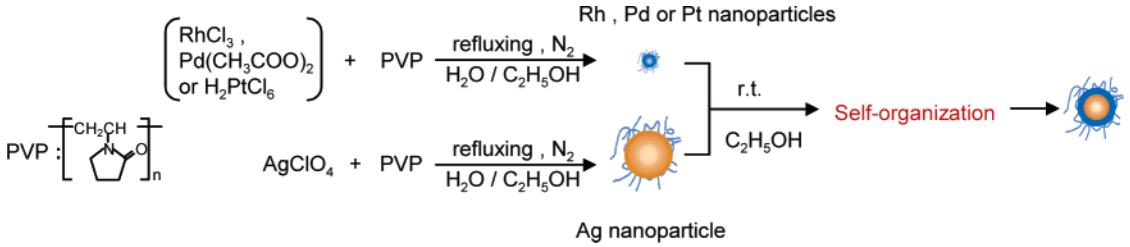

Figure 1. Process of spontaneous formation of bimetallic nanoparticles by mixing of two kinds of monometallic nanoparticles prepared independently by refluxing in water/ethanol. Colloidal dispersion of Ag nanoparticles and noble metal nanoparticles in ethanol just mixed at room temperature. The mixtures were kept at room temperature, resulting in colloidal dispersion of bimetallic nanoparticles by self-organization.

Experimental Section

Materials. Silver perchlorate and palladium(II) acetate were used as supplied by Kojima Chemicals Co., Ltd. and rhodium(III) chloride, hexachloroplatinic(IV) acid, and ethanol by Wako Pure Chemical Industries, Ltd. Poly(*N*-vinyl-2-pyrrolidone) (PVP, K-30, average molecular weight 40 000; Wako Pure Chemical, Industries, Ltd.) was used without further purification as the protective polymer for the product metal nanoparticles.

Preparation of Metal Nanoparticles.[38] A typical procedure to prepare polymer-protected monometallic nanoparticles is as follows: A solution of noble-metal salts (silver perchlorate, rhodium(III) chloride, palladium(II) acetate, or hexachloroplatinic(IV) acid) (0.66 mM) in 500 mL of ethanol/water (1/9, v/v) was heated with refluxing for a few hours under nitrogen in the presence of PVP (13.2 mmol) as protecting polymer. Ethanol serves as a reducing agent. PVP-protected metal nanoparticles thus prepared were purified by filtration with ultrafilter (Advantec, Q0100076E) and by washing with degassed and deionized water to remove byproduced ions, and then dried under vacuum. The dried metal nanoparticles were dispersed in pure ethanol under nitrogen. The ratio *R* of the amount of PVP present in solution over that of metal ions was generally fixed at 40. When the ratio *R* is reduced to 5 for Ag, the average diameter of the resultant Ag particles increased. We call this Ag nanoparticle Ag(L). For the Ag nanoparticle prepared with the ratio *R* of standard 40, which we call Ag(S), the particle size was about half that of Ag(L). Dispersions of the Ag and noble metal (Rh, Pd, or Pt) nanoparticles that were prepared separately with the same concentration of PVP were mixed to form bimetallic nanoparticles at room temperature. We follow this process depicted in Figure 1 by ITC.

Measurements. Ultraviolet and visible (UV−vis) spectra were obtained at room temperature using a Shimadzu 2500PC recording spectrophotometer equipped with a 10 mm quartz cell. Transmission electron microscopy (TEM), a JEOL JEM-1230 electron microscope operated at 80 kV, was used to characterize the monometallic and bimetallic nanoparticles. Samples for TEM measurement were prepared by placing a drop of the colloidal dispersion of metal nanoparticles onto a carbon-coated copper microgrid, followed by naturally evaporating the solvent. The mean diameter and standard deviation were calculated by counting the diameters of ca. 200 particles with a magnifier (10 times) on the TEM photograph of 100 000 magnification.

Isothermal titration calorimetric (ITC) experiments were performed using a MicroCal MCS-ITC instrument at 30 °C, wherein 50 μL of a 0.66 mM ethanol solution of metal nanoparticles dispersion was injected in equal steps of 2.5 μL into 1.34 mL of a 0.66 mM ethanol solution of another nanoparticle dispersion. All the samples used for calorimetric measurement were purified by removing the byproducts, produced during the preparation of monometallic nanoparticles, with a ultrafilter separation system (Advantec, UHP-76K). For Ag(L), the concentration of PVP was adjusted to the ratio *R* value of 40. In this manner, the background due to any possible dilution effect of PVP in ethanol became negligible as shown below.

Results and Discussion

Formation of Core/Shell-Structured Bimetallic Nanoparticles by Mixing Dispersions of the Corresponding Two Kinds of Monometallic Nanoparticles. Reduction of metal ions to dispersions of monometallic nanoparticles was confirmed by the disappearance of bands attributed to metal ions and the appearance of tailing bands attributed to reflection of metal nanoparticles or of the plasmon band in the case of Ag nanoparticles in UV−vis absorption spectra. TEM observation indicated the product nanoparticles are reasonably monodispersed as shown in Figure 2. The average diameters are 22.5, 10.6, 2.4, 2.3, and 2.4 nm respectively for Ag(L), Ag(S), Rh, Pd, and Pt nanoparticles. The size distribution histograms of the nanoparticles are also shown in Figure 2.

Figure 3 shows the UV−vis spectra as a function of time when Ag and other metal nanoparticle dispersions were mixed at room temperature. The 420 nm surface plasmon peak due to Ag nanoparticles gradually disappeared on standing with varying time constants. This observation suggests that the surface of Ag nanoparticles (b in Figure 4) is covered with Rh nanoparticles (a in Figure 4) to form bimetallic nanoparticles of pseudo-core/shell (c in Figure 4). This kind of assembly was also observed in TEM photographs after mixing Ag and Rh nanoparticles.[25] Recently we found that the aggregate structures can be rearranged just by keeping the mixed dispersions for a few days at room temperature to form a reasonably monodispersed bimetallic nanoparticle of the true core/shell structure (d in Figure 4) with a smaller size than the original Ag nanoparticles. Details will be published elsewhere.

Calorimetric Measurement of an Interaction between Silver and Other Noble Metal Nanoparticles. For the formation of bimetallic nanoparticles of pseudo-core/shell, as shown in Figure 4c, the first step of the reaction should be an interaction between the two monometallic nanoparticles. Thus, we evaluate the degree of interaction between the two by isothermal titration calorimetric (ITC) measurements.

For this purpose, an amount of the alcoholic dispersion of PVP-protected nanoparticles of a noble metal like Rh, Pd, or Pt was titrated successively into the alcoholic dispersion of PVP-protected Ag(S) nanoparticles. As mentioned above, we made the concentration of the alcoholic solution with PVP the same. As shown in Table 1, the background signal due to any possible dilution effect of the dispersion solution is negligible in comparison with the interaction between different metal nanoparticles shown in Table 2. Figure 5a shows the heat flow trace as successively titrating the PVP-protected Pd nanoparticle dispersion into the Ag(S) dispersion. As is evident from the

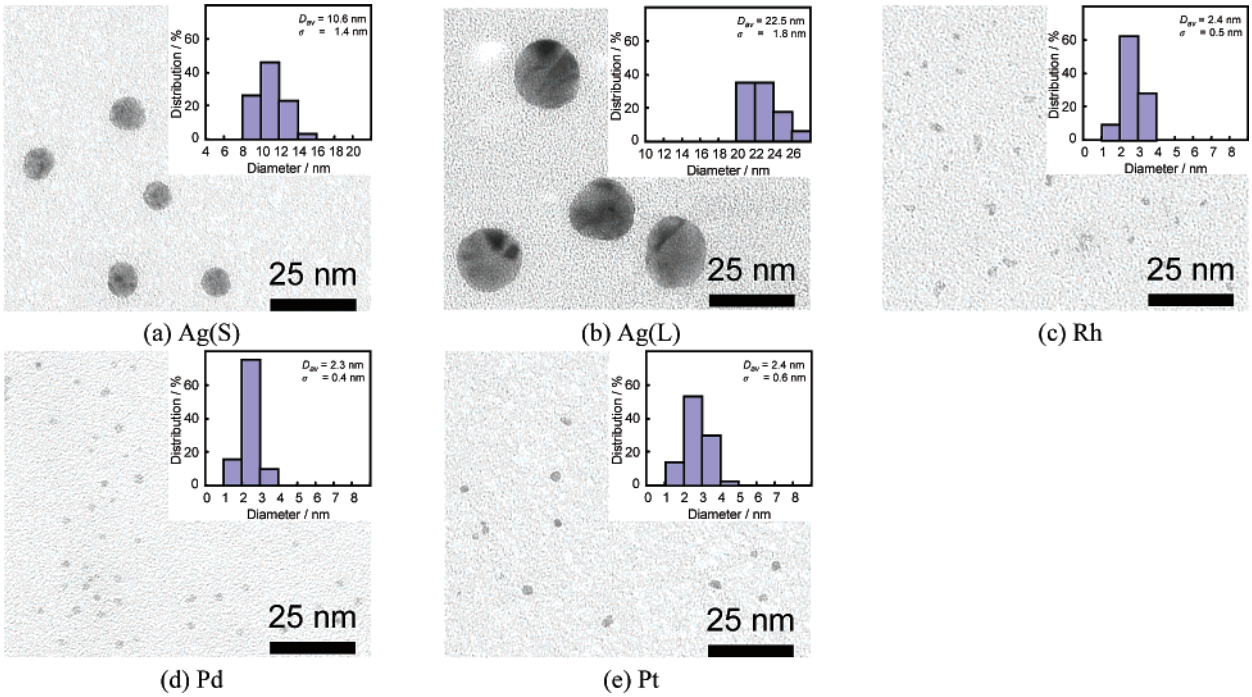

Figure 2. Transmission electron micrographs and particle size distribution histograms of noble metal nanoparticles: (a) PVP−Ag(S), (b) PVP−Ag(L), (c) PVP−Rh, (d) PVP−Pd, and (e) PVP−Pt. D_{av} = average diameter, σ = standard deviation.

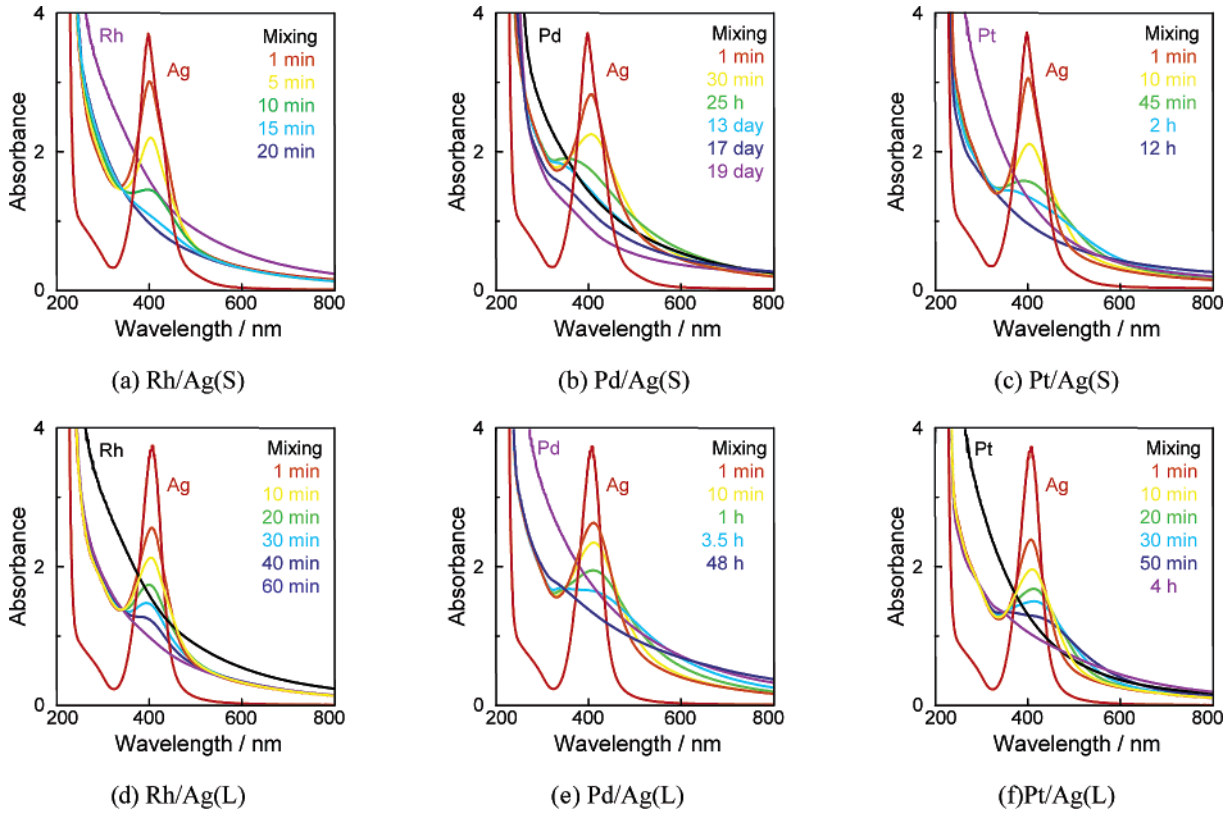

Figure 3. UV−vis spectral change of the mixtures of colloidal dispersions of Ag and noble metal nanoparticles. The original Ag surface plasmon absorption peak was quenched by keeping the mixed solution at room temperature after the addition of noble metal nanoparticles.

figure, the return of the peak signal to the baseline seems satisfactory. This ensures appropriate operation of ITC for the present colloid−colloid interactions. Indeed, when the volume of each titrant is increased to 10 μL, it took more than 30 min for the peak to return to the baseline. Hence we chose 2.5 μL for the volume of titrant. In Figure 5b the area of each peak shown in Figure 5a is converted to the enthalpy change induced per mole of metal of the injectant. The abscissa shows the molar ratio of the total number of moles of injected metal over that of the titrate in the cell. As is typical for ITC in general, the first data point is always undersize due to dilution of the sample at the tip of the syringe needle. As shown in Figure 5a, it requires a few more shots before the peak size settles down. When we reversed titration, i.e., titration of Ag(S) or Ag(L) into Rh, Pd, or Pt, a few more data points than in the above cases are required as shown in Figure 5d. Our experience of titrating a solution of

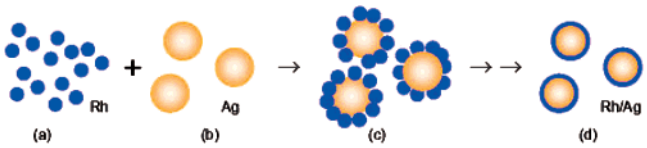

Figure 4. Schematic presentation of formation of core/shell structure (d) by mixing Rh (a) and Ag (b) nanoparticles through pseudo-core/shell structure (a), where Rh nanoparticles surround Ag nanoparticles.

TABLE 1: Molar Enthalpy Obtained with ITC by Injecting a Particle Dispersion into the Same Particle Dispersion

injection particles[a]		particles in cell[a]	ΔH (kJ/mol)
PVP−Ag	→	PVP + ethanol	−4.2
PVP−Rh	→	PVP−Rh	−5.9
PVP−Pd	→	PVP−Pd	−1.1
PVP−Pt	→	PVP−Pt	0.5
PVP−Ag(S)	→	PVP−Ag(S)	1.7
PVP−Ag(L)	→	PVP−Ag(L)	3.6
PVP−Ag(L)	→	PVP−Ag(S)	−1.3
PVP−Ag(S)	→	PVP−Ag(L)	2.9

[a] Particle size is given in parentheses.

biopolymers indicates that initial multiple injections are necessary at times. This may hint that some rheological complication might be at work in the narrow space of the syringe needle, and a number of shots of titration may be necessary to reach a steady state so that a constant volume is delivered. The colloidal dispersions are indeed notorious in this respect, and are more complex for dispersion of large colloidal particles.[39,40] This could explain why a few more initial data points are required for Ag-(L) than for Ag(S). While we have no precise reason for this observation, we ignore the first several points and extrapolate the remaining data linearly as shown in Figure 5, panel b or d, to evaluate the enthalpy change per mole of metal in the injectant at the zero molar ratio, i.e., at the very first contact between two metals.

The results are shown in Tables 1 and 2. Table 1 summarizes the results for enthalpic values for "the background". It is evident that the background values are negligibly small in comparison

TABLE 2: Molar Enthalpy Obtained with ITC by Injecting a Particle Dispersion into Another Particle Dispersion

entry no.	injection particles[a]		particles in cell[a]	ΔH (kJ/mol)	$\Delta H \times 10^{27}$ (J/particle)
1	PVP−Rh	→	PVP−Ag(S)	−908	−0.79
2	PVP−Pd	→	PVP−Ag(S)	−600	−0.43
3	PVP−Pt	→	PVP−Ag(S)	−278	−0.22
4	PVP−Rh	→	PVP−Ag(L)	−963	−0.84
5	PVP−Pd	→	PVP−Ag(L)	−1093	−0.78
6	PVP−Pt	→	PVP−Ag(L)	−628	−0.50
7	PVP−Ag(S)	→	PVP−Rh	−357	−21.6
8	PVP−Ag(S)	→	PVP−Pd	−331	−21.2
9	PVP−Ag(S)	→	PVP−Pt	−189	−11.4
10	PVP−Ag(L)	→	PVP−Rh	−395	−228
11	PVP−Ag(L)	→	PVP−Pd	−403	−234
12	PVP−Ag(L)	→	PVP−Pt	−223	−130

[a] Particle size is given in parentheses.

with the data shown in Table 2. The values in Table 2 show that the first contact interaction between two sets of metal nanoparticles is indeed strongly exothermic and apparently in the order of Rh/Ag > Pd/Ag > Pt/Ag.

We note in Table 2 that the enthalpy change at the ratio zero diminishes by several fold on reversing the titrant and the titrate. This could be due to the size difference between Ag(L or S) and noble metal (Rh, Pd, or Pt) nanoparticles. The enthalpy change ΔH is given as the value per mole of the injectant metal. Clearly there are a larger number of particles in a given mole of metal atom if the particle size is smaller. Therefore more appropriate data should be expressed as an enthalpic value per particle of the titrant, which we calculated using the average particle size in Figure 2, and assuming that the density of nanoparticle is the same as that of bulk metal. Indeed, as we showed earlier by XRD diffractograms and/or HRTEM micrographs,[41] the density of metal nanoparticles can be regarded as roughly the same as that of bulk metals.

The last column of Table 2 shows the results. The values for titrating the suspension of small noble metal particles into that of large Ag particles, Nos. 1 to 6, and those for the reverse case, Nos. 7 to 12, are different by some several fold. This is,

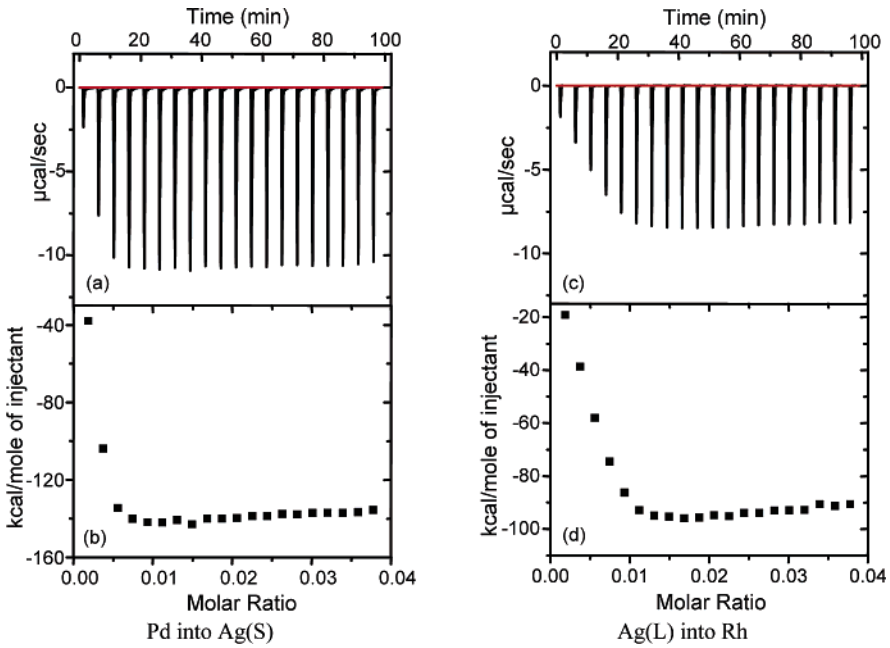

Figure 5. The calorific value per time at the time of titration of (a) PVP-protected Pd nanoparticles into PVP-protected Ag(S) nanoparticles and (c) PVP-protected Ag(L) nanoparticles into PVP-protected Rh nanoparticles, and (b and d) the enthalpy changes induced per mole of the injectants, respectively.

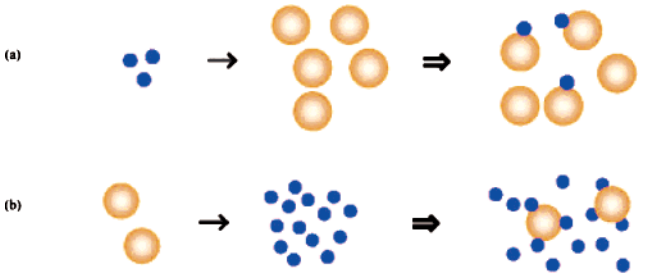

Figure 6. Schematic presentation of the initial state of a reaction in calorimetric measurement: (a) injecting Rh small nanoparticle dispersion into Ag large nanoparticle dispersion and (b) injecting Ag large nanoparticle dispersion into Rh small nanoparticle dispersion.

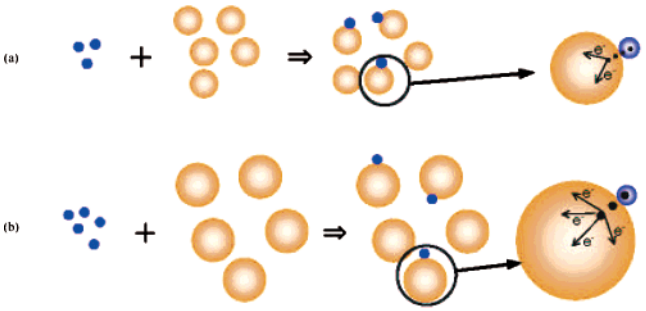

Figure 7. Schematic presentation of the initial state of a reaction in calorimetric measurement: (a) injecting small noble metal nanoparticles into Ag small nanoparticles and (b) injecting small noble metal nanoparticles into Ag large nanoparticles.

however, not surprising. At the zero mole ratio, an infinitely small number of particles are injected into the suspension of the infinitely large number of particles of the titrate in the cell. If the size of the injectant particle is smaller than that in the cell, one to one contact is very likely as shown in Figure 6a. For the reverse situation as in Figure 6b, it is more likely that a number of small particles interact with a single large particle.

Hence, the enthalpic values in the last column of Table 2 for cases of small particle titrant, Nos. 1 to 6, could represent the one-to-one interaction between the pair of metal nanoparticles. Then, the values for runs for Nos. 7 to 12 could provide a crude estimate for the number of small particles that interact with a single large Ag particle. For the Ag(S) sample, this number ranges from 20 to 30, while for Ag(L), it is about 250. This is about $^1/_3$ to $^1/_2$ of the full monolayer coverage assuming the above picture, Figure 6, is reasonable. Turning back to the enthalpy values per particle, which represents the true one-to-one interaction between the two metal nanoparticles, it is also evident that the interaction is exothermic and in the order of Rh/Ag > Pd/Ag > Pt/Ag. This order is interesting. It looks like the order of ionization potential of noble metals. (The ionization potentials of Rh, Pd, and Pt are 7.46, 8.34, and 9.00 eV, respectively.) However, the electronic states of nanoparticles are not the same as those in atom, nor in metal. Also it is highly dependent on size. In fact, this order is not correct in the case of large Ag nanoparticles. Thus, we have no exact explanation for the observed ranking. No doubt, however, this result will help in understanding the electronic state of these nanoparticles.

Is there a significant difference between Ag(L) and Ag(S), No. 1 vs No. 4, No. 2 vs No. 5, and No. 3 vs No. 6? The one-to-one enthalpy for Ag(L) is somewhat larger than that for Ag(S). We may speculate this to be due to more room for accommodating electron charges to Ag(L) than to Ag(S). This concept can be schematically presented in Figure 7. Thus, when a tiny noble metal nanoparticle, blue ball in Figure 7, comes in contact with a small Ag nanoparticle, orange ball in Figure 7 (case a), the change of the electronic state of the Ag nanoparticle by contact with a noble metal nanoparticle may diffuse from the place of contact into the whole ball. However, this diffusion may be limited by the small size of the Ag nanoparticle. In the case of a large Ag nanoparticle (case b), in contrast, this diffusion may spread out into the large nanoparticle.

TABLE 3: Molar Enthalpy Obtained with ITC by Injecting a Particle Dispersion into Another Particle Dispersion

entry no.	injection particles		particles in cell	ΔH (kJ/mol)
13	PVP−Pt	→	PVP−Pd	−289
14	PVP−Pd	→	PVP−Pt	−219
15	PVP−Pt	→	PVP−Rh	−262
16	PVP−Rh	→	PVP−Pt	−180
17	PVP−Pd	→	PVP−Rh	−107
18	PVP− Rh	→	PVP−Pd	−97

Calorimetric Measurement of an Interaction between Noble Metal Nanoparticles. So far we discussed the reaction/interaction between Ag and another kind of noble metal nanoparticle. What about the interaction between a pair of noble metal nanoparticles themselves? Table 3 shows the results of ITC studies. Surprisingly all the cases show exothermic interactions in the order of Pt/Pd > Pt/Rh > Pd/Rh.

While the nature of nanoparticle pairing among these noble metals should be investigated further, we stress the sensitivity of ITC in detecting the interactions among them, which were not realized so far. The present findings will no doubt lead to further investigations on noble metal nanoparticle paring for potential applications in nanotechnologies.

Conclusion

Spontaneous formation of bimetallic core/shell nanoparticles[25] by mixing the dispersion of poly(*N*-vinyl-2-pyrrolidone) (PVP)-protected Ag nanoparticles with that of PVP-protected noble metals (Rh, Pd, and Pt) in ethanol at room temperature was confirmed here by the disappearance of the plasmon absorption of Ag with time. Furthermore, isothermal titration calorimetric (ITC) measurements revealed the strong exothermic interaction between Ag nanoparticles and noble metal nanoparticles. The strength of the interaction between a pair of metals increases in the order of Ag/Pt < Ag/Pd < Ag/Rh. This strong exothermic interaction is no doubt a driving force for spontaneous formation of bimetallic nanoparticles with a low-entropy pseudo-core/shell structure. Similar exothermic interactions were also observed between a pair of noble metal (Rh, Pd, and Pt) nanoparticles. We applied ITC technique for the first time to determine the degree of interaction/reaction between metal nanoparticles, and demonstrated its utility and sensitivity for studies in nanoparticle science. Thus, ITC should be added to a long list of experimental techniques that are useful in nanoparticle investigations.

Acknowledgment. This work was supported by a Grant-in-Aid for Scientific Research (B) (No. 15310078) by the Ministry of Education, Culture, Sports, Science and Technology (MEXT) of the Japanese Government. We thank Professor Peter Westh for helpful discussion regarding some difficulty in a few initial titrations in ITC.

References and Notes

(1) De Jongh, L. J., Ed. *Physics and Chemistry of Metal Cluster Compounds*; Kluwer Academic/Plenum Publishers: Dordrecht, The Netherlands, 1994.

(2) Schmid, G., Ed. *Clusters and Colloids From Theory to Applications*; VCH: Weinheim, Germany, 1994.

(3) Fendler, J. H., Ed. *Nanoparticles and Nanostructured Films*; Wiley-VCH: Weinheim, Germany, 1998.

(4) Sugimoto, T., Ed. *Fine Particles*: *Synthesis, Characterizations, and Mechanisms of Growth*: Marcel Dekker: NewYork, 2000.

(5) Liz-Marzan, L. M.; Kamat, P. V., Eds. *Nanoscale Materials*; Kluwer Academic/Plenum Publishers: Boston, MA, 2003.

(6) Toshima, N. *Encyclopedia of Nanoscience and Nanotechnology*; Scwarz, J. A., Contescu, C., Putyera, K., Eds.; Marcel Dekker: New York, 2004; p 1869.

(7) Yonezawa, T., Ed. *Metal Nanoparticles*: *Synthesis, Preparation Control Technology, and Applications*; Gijutsu Joho Kyokai: Tokyo, Japan, 2004.

(8) Toshima, N.; Yonezawa, T. *New J. Chem*. **1998**, *22*, 1179.

(9) Teranishi, T.; Toshima, N. *Catalysis and Electrocatalysis at Nanoparticle Surfaces*; Wieckowski, A., Sarimone, E. R., Vayenas, C. C., Eds.; Marcel Dekker: New York, 2003; Chapter 11, p 379.

(10) Toshima, N. *Macromolecular Nanostructured Materials*; Ueyama, N., Harada, A., Eds.; Kodansha/Springer: Tokyo, Japan/Berlin, Germany, 2004; Chapter 3.3, p 182.

(11) Toshima, N.; Kushihashi, K.; Yonezawa, T.; Hirai, H. *Chem. Lett*. **1989**, 1769.

(12) Toshima, N.; Yonezawa, T.; Kushihashi, K. *J. Chem. Soc., Faraday Trans.* **1993**, *89*, 2537.

(13) Toshima, N. *Nanoscale Materials*; Liz-Margen, L. M., Kamat, P. V., Eds.; Kluwer Academic/Plenum Publishers: Berlin, Germany, 2003; pp 79−96.

(14) Bian, C.-R.; Suzuki, S.; Asakura, K.; Lu, P.; Toshima, N. *J. Phys. Chem. B* **2002**, *106*, 8587.

(15) Toshima, N.; Harada, M.; Yonezawa, T.; Kushihashi, K.; Asakura, K. *J. Phys. Chem*. **1991**, *95*, 7448.

(16) Harada, M.; Asakura, K.; Ueki, Y.; Toshima, N. *J. Phys. Chem.* **1992**, *96*, 9730.

(17) Toshima, N.; Harada, M.; Yamazaki, Y.; Asakura, K. *J. Phys. Chem.* **1992**, *96*, 9927.

(18) Yonezawa, T.; Toshima, N. *J. Mol. Catal*. **1993**, *83*, 167.

(19) Mizukoshi, Y.; Fujimoto, T.; Nagata, Y.; Oshima, R.; Maeda, Y. *J. Phys. Chem. B* **2000**, *104*, 6028.

(20) Kan, C.; Cai, W.; Li, C.; Zhang, L.; Hofmeister, H. *J. Phys. D*: *Appl. Phys*. **2003**, *36*, 1609.

(21) Mandal, S.; Mandale, A. B.; Sastry, M. *J. Mater. Chem*. **2004**, *14*, 2868.

(22) Tada, H.; Suzuki, F.; Ito, S.; Akita, T.; Tanaka, K.; Kawahara, T.; Kobayashi, H. *J. Phys. Chem. B* **2002**, *106*, 8714.

(23) Hodak, J. H.; Henglein, A.; Hartland, G. V. *J. Chem. Phys*. **2001**, *114*, 2760.

(24) Wang, Y.; Toshima, N. *J. Phys. Chem. B* **1997**, *101*, 5301.

(25) Hirakawa, K.; Toshima, N. *Chem. Lett.* **2003**, *32*, 78.

(26) Makishima, S. *Pattern Dynamics*: *A Theory of Self-Organization*; Kodansha Scientific: Tokyo, Japan, 2001.

(27) Harrison, L. G. *Kinetic Theory of Living Pattern*; Cambridge University Press: New York, 1993.

(28) Bloor, D. M.; Wyn-Jones, E., Eds. *Structure, Dynamics, and Equilibrium Properties of Colloidal Systems*; NATO ASI series, Ser. C; Kluwer Academic/Plenum Publishers: Dordrect, The Netherlands, 1990; Vol. 324.

(29) Sollich, P. *J. Phys*.: *Condens. Matter* **2002**, *14*, R79−R117.

(30) Jelesarov, I.; Bosshard, H. R. *J. Mol. Recognit*. **1999**, *12*, 3.

(31) Thompson, G.; Owen, D.; Chalk, P. A.; Lowe, P. N. *Biochemistry* **1998**, *37*, 7885.

(32) Wenk, M. R.; Seelig, J. *Biochemistry* **1998**, *37*, 3939.

(33) Zhang, Y.; Akhilesh, S.; Wilcox, D. E. *Inorg. Chem*. **2000**, *39*, 3057.

(34) Tellez-Sanz, R.; Garcia-Fuentes, L.; Baron, C. *FRBS Lett*. **1998**, *423*, 75.

(35) Gouriskaukar, A.; Shukle, S.; Ganesh, N. K.; Sastry, M. *J. Am. Chem. Soc*. **2004**, *126*, 13186.

(36) Joshi, H.; Shirude, P. S.; Bansal, V.; Ganesh, K. N.; Sastry, M. *J. Phys. Chem. B* **2004**, *108*, 11535.

(37) Kanemaru, M.; Shiraishi, Y.; Koga, Y.; Toshima, N. *J. Therm. Anal. Calorim.* **2005**, in press.

(38) Hirai, H.; Nakao, Y.; Toshima, N. *J. Macromol. Sci. Chem.* **1979**, *A13*, 727.

(39) Wu, H.-J.; Bevan, M. A. *Langmuir* **2005**, *21*, 1244.

(40) Thwar, P. K.; Velegal, D. *Langmuir* **2002**, *18*, 7328.

(41) Lu, P.; Teranishi, T.; Asakura, K.; Miyake, M.; Toshima, N. *J. Phys. Chem. B* **1999**, *103*, 9673.